

# **EFFECT OF Nb MICROALLOYING ON THE HEAT AFFECTED ZONE MICROSTRUCTURE OF X80 LARGE DIAMETER PIPELINE AFTER IN-FIELD GIRTH WELDING**

M. Guagnelli, A. Di Schino, M. C. Cesile and M. Pontremoli

Centro Sviluppo Materiali SpA, Via di Castel Romano 100, 00128 Rome, Italy

Keywords: Niobium, Microstructure, Mechanical Properties

## **Abstract**

The effect of Nb content in the range 0.07%-0.10% on the HAZ microstructure of X80 large diameter pipes is reported in this paper. Results show that, despite the difference in Nb content, no differences have been found in the prior austenitic grain size and consequently in the local hardenability. On the other hand, Nb is able to influence the size of the bainitic packets and cells in the heat affected zone, i.e. the microstructural parameters affecting impact toughness and hardness behavior. Such an effect leads to an improvement of both toughness and hardness for the steel with higher Nb content.

## **Introduction**

The development of steels for linepipes during the last decades has been driven by the need to obtain improved combinations of high strength, toughness and weldability on an industrial scale at affordable prices. A similar situation occurred in other fields of application of structural steels, like offshore steel structures or ships, with broadly similar objectives, even though the balance of requirements could vary depending on the specific design or operational needs.

Niobium, with its specific thermodynamic and kinetic aptitude to form carbide and nitride precipitates, played a key role in the development of modern, controlled processed HSLA steels. These steels have certainly made possible the efficient and cost-effective design and the development of construction technologies in a variety of applications. In the field of transportation pipelines, for example, the increase in the available strength level of linepipe that has taken place during the last forty years (from X52 to X100) has produced cumulative benefits valued in the billion dollar range, largely because they have been achieved without compromising construction methods that were prevalent in the industry.

The effect of niobium on the microstructure and the properties of the heat affected zone (HAZ) of a girth weld is a very complex issue because of a number of different interrelated mechanisms which also depend on the chemical composition of the steel and on the welding parameters.

In particular it is known that:

- undissolved precipitates (typically complex (Ti,Nb)(C,N)) have a significant effect on austenite grain size [1, 2, 3]. It is well known that austenite grain size affects the hardenability of the steel and has consequently [4, 5] an influence on the toughness through the packet size of the final microstructure;
- Nb in solid solution has a direct impact on the hardenability by reducing the transformation temperature of the austenite [6];
- Nb carbonitrides may precipitate in ferrite with a consequent impact on strength and toughness.

Despite the importance of Nb in the development of high strength pipelines with good toughness, possible detrimental effects on the properties of the HAZ of welded joints are reported in the literature (in particular concerning toughness) [7]. For this reason, in the past decades niobium content has been often limited up to about 0.05 percent. However, recently a new generation of higher (up to about 0.1%) niobium pipeline steels has been developed and produced for high pressure long distance gas transportation, and such linepipes passed the qualification process, indicating the suitability of the higher niobium concept.

The aim of this paper is to investigate the effect of Nb addition up to 0.10% on HAZ microstructure and mechanical properties of X80 large diameter linepipes.

### Materials and Experimental Details

X80 pipes manufactured from the steels reported in Table I were considered. The steels have similar chemical composition, apart from Nb content, 0.07%-0.10%, and Mo (0.10%-0.25%).

Table I. Chemical Composition of the Considered Steels (mass, %)

|               | C, % | Mn, % | Si, % | Ni, % | Cr, % | Mo, % | Nb, % | Ti, % | Al, % |
|---------------|------|-------|-------|-------|-------|-------|-------|-------|-------|
| <b>Pipe A</b> | 0.04 | 1.83  | 0.18  | 0.25  | 0.26  | 0.10  | 0.07  | 0.013 | 0.032 |
| <b>Pipe B</b> | 0.04 | 1.75  | 0.24  | 0.26  | 0.23  | 0.25  | 0.10  | 0.018 | 0.028 |

Pipe A is longitudinally welded (manufactured from plate) while pipe B is helically welded (manufactured from coil).

The microstructure was observed by means of Light Microscopy (LM) on polished sections after 2% Nital etching.

Packet size was determined by Image Orientation Microscopy (OIM) technique using electron back-scattering diffraction (EBSD) pattern. By means of this technique, the surface of a crystalline material with low dislocation density can be scanned and for each point the orientation of the underlying grain can be determined in a fully automatic way. From these measurements some microstructural characteristics of the material can be estimated, e.g. misorientations between adjacent crystallographic orientations, etc. It is of great importance to assess the crystallographic grain size, because this parameter greatly influences the strength and the cleavage fracture resistance of ferritic steels. EBSD is a very helpful method to measure the

effective grain size, even for fine microstructures. The term “packet size” is employed here for the effective grain size, whatever the phase in question.

Precipitation state was examined by TEM extraction replicas in a JEOL JEM 3200FS-HR scanning transmission electron microscope operating at 300 kV with a JEOL EDS microanalysis system. The latter was equipped with a Si detector, with a resolution of 139 eV FWHM for the  $K\alpha$  line of Mn (5.89 keV), and automatic image analysis software for feature sizing of particles, able to measure various geometrical parameters of precipitates. Quantitative EDS analysis with high spatial resolution was performed using the Cliff-Lorimer method. More than 2000 particles were measured for each size distribution. Precipitate size ( $d_p$ ) was considered. The measurements were carried out at low magnification (20,000X) for particles greater than 100 nm, and at high magnification (100,000X) for particles smaller than 100 nm, respectively.

In order to compare the precipitate morphology, the following parameter was measured:

$$\text{Shape factor (circularity)} = \frac{4\pi A}{P^2} \quad (1)$$

where A is the area of the particle and P its perimeter. This parameter is equal to 1 for round particles and is lower than 1 for elongated ones. The shape factor was calculated for precipitates smaller than 300 nm. At least 50 particles were used to investigate the chemical analysis of precipitates, using a lifetime for the acquisition of the X-ray peaks by EDS longer than 50 s.

Tensile testing was performed on full thickness cross weld specimens.

Charpy-V notch testing was conducted on transverse specimens with the notch at the fusion line. Charpy-V transition curves were determined together with the fracture appearance transition temperature (50% FATT).

## Results

### Microstructure and Precipitation of the Base Materials

The microstructure of the base material of both pipes A and B is shown in Figure 1. Both pipes are characterized by a fine acicular ferrite microstructure typical of X80 grades; pipe A shows a coarser microstructure (larger packet size) with a visible pancaking feature typical of plate rolling.

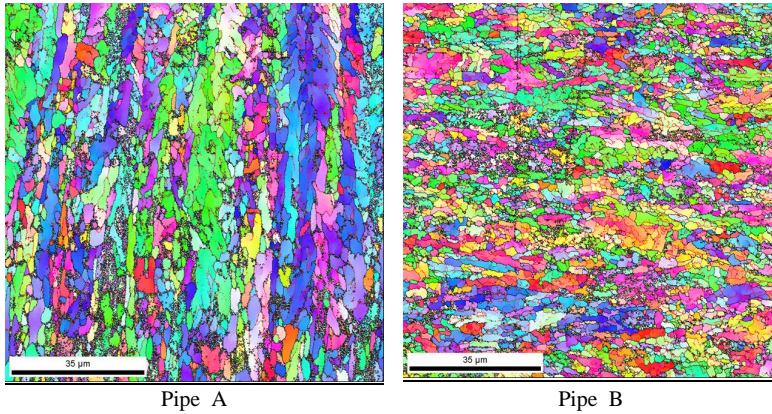


Figure 1. General view of microstructure of pipes A and B by EBSD.

Precipitates are mainly Nb/Ti carbides in both materials. The precipitation state, as revealed by the observation of carbon replicas by TEM, shows that in both steels a population of coarse particles with size greater than about 100 nm is present. In addition, in steel B, also a relevant number of finer particles can be observed, Figure 2.

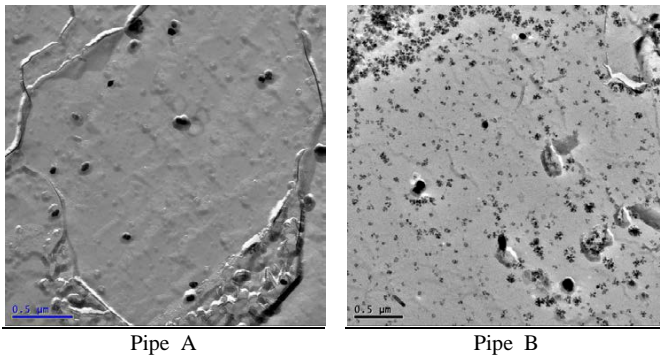
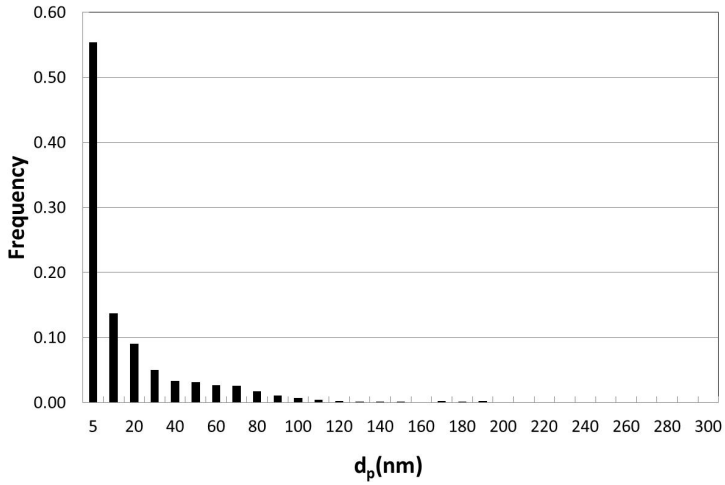
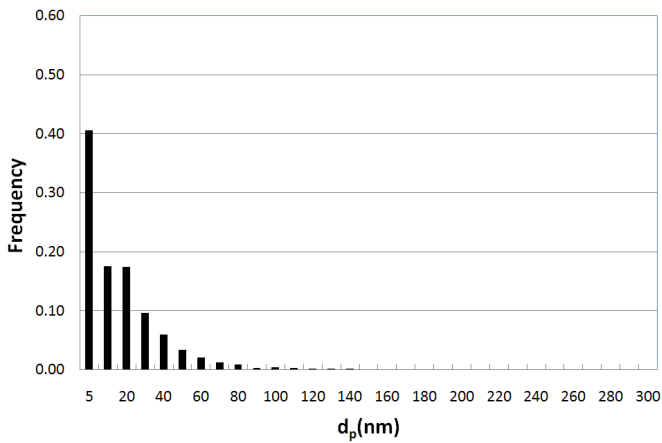


Figure 2. General view of precipitation state in the base metal of pipes A and B by TEM extraction replica.



Pipe A

Figure 3a. Precipitate size distributions in the base metal of pipe A determined by automatic image analysis of particle diameter on carbon extraction replicas by TEM.



Pipe B

Figure 3b. Precipitate size distributions in the base metal of pipe B determined by automatic image analysis of particle diameter on carbon extraction replicas by TEM.

The precipitate size distributions determined by automatic image analysis on carbon extraction replicas are reported in Figure 3. By evaluating the average precipitate size it is clearly observed that particles are finer in steel B, Table II. In both cases precipitates are almost spherical, as confirmed by values of the shape factor higher than 0.80.

Generally speaking, in steels microalloyed with both Ti and Nb, it is expected that smaller particles are richer in Nb and the larger in Ti, according to the precipitation sequence as a function of temperature. This feature is present in the plot of precipitate composition of steel A in Figure 4 but it is not apparent in that of steel B, where the particles are generally richer in Nb, irrespective of their size.

Table II. Average Precipitate Size and Shape Factor in the Base Metal of Pipes A and B

|               | $d_p$ (nm) | Shape factor |
|---------------|------------|--------------|
| <b>Pipe A</b> | 56.5       | 0.82         |
| <b>Pipe B</b> | 16.0       | 0.85         |

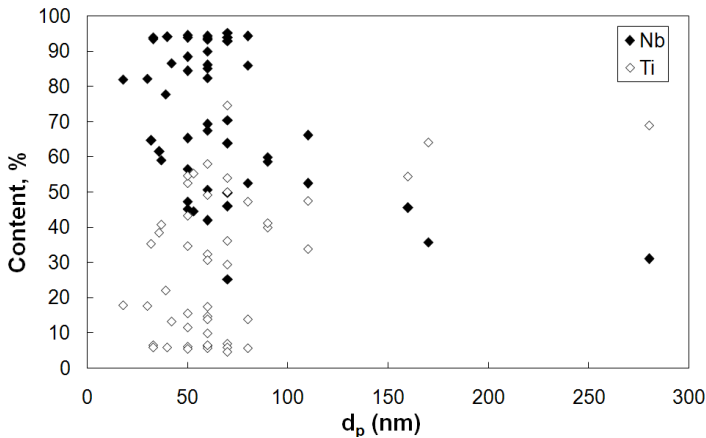


Figure 4a. Content of Nb and Ti in carbonitrides (expressed as atomic percent in the metallic sublattice) as a function of the precipitate size, pipe A.

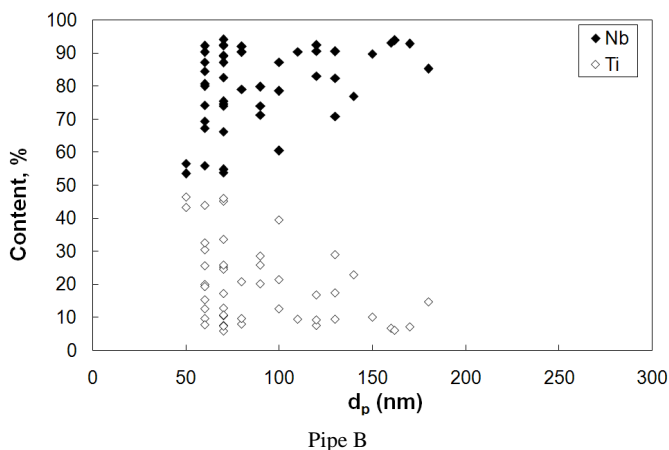


Figure 4b. Content of Nb and Ti in carbonitrides (*expressed as atomic percent in the metallic sublattice*) as a function of the precipitate size, pipe B.

### Microstructure in HAZ

The general aspect of the microstructure of welded joints is shown in Figure 5. EBSD images show the microstructure variation from weld metal to base material in steels A and B. The microstructure appears to be constituted by acicular ferrite. The results show that the increase of Nb content from 0.07% to 0.10% reduces the CGHAZ extent (from 275  $\mu\text{m}$  down to 125  $\mu\text{m}$ ). Moreover, a finer microstructure (finer packet size) is found in steel B (higher Nb content) with respect to steel A in the CGHAZ region, Figure 6. On the contrary, no significant differences are detected in the prior austenite grain size which was found to range between 25 and 30  $\mu\text{m}$  in both cases, Figure 7.

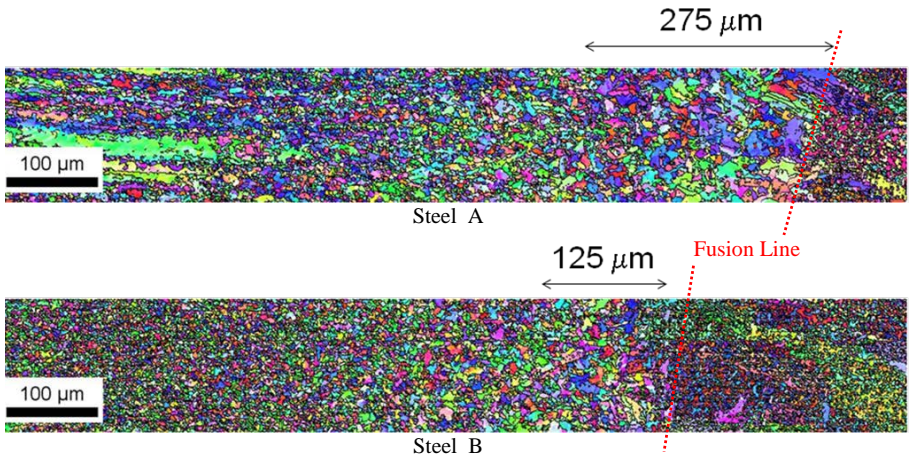


Figure 5. General view of the weld joint microstructure by EBSD.

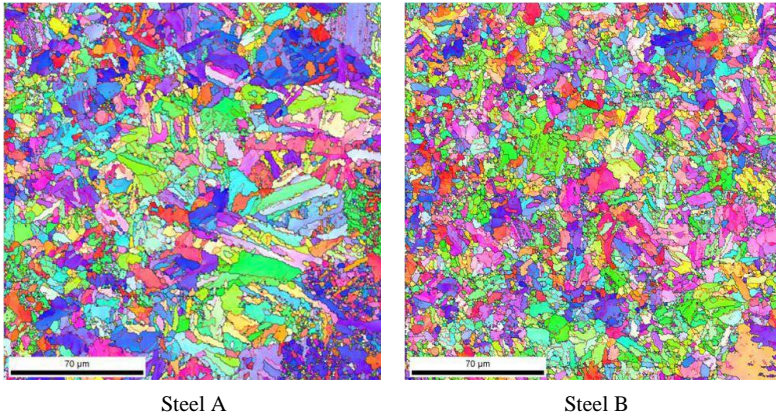
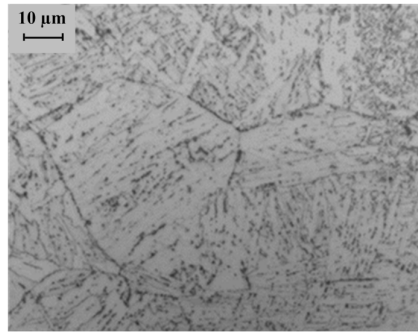
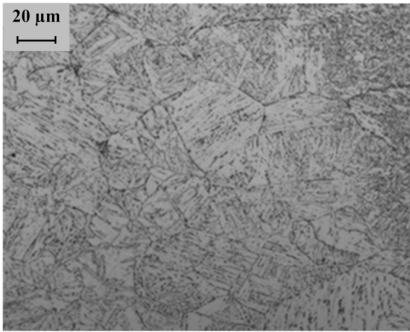
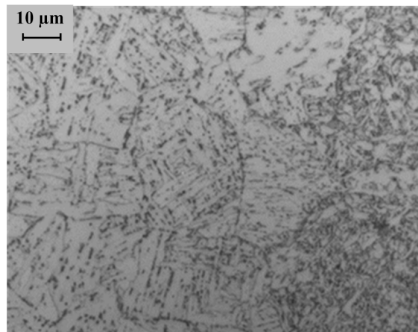
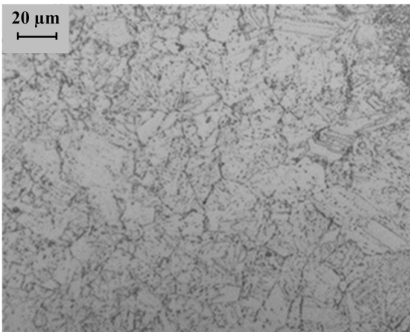


Figure 6. Microstructure in CGHAZ by EBSD.



**Steel A**



**Steel B**

Figure 7. Microstructure in CGHAZ by LM (2% Nital etching).

The almost perfect superposition between the misorientation distributions determined by EBSD, Figure 8, indicates that, also at the level of sub-grains, there are no significant differences in the mechanisms of austenite decomposition as far as the microstructure as a whole is concerned.

Instead, the finer microstructure in the steel with higher Nb content might be explained by the following mechanism. The austenite grain size in the HAZ is not affected by the Nb content because there is a similar fraction of coarse particles present in both steels, which did not dissolve completely during the reheating stage of welding, and limited the growth of austenite grains by exerting an effective pinning on their boundaries. In the mean time, a certain fraction of carbides, especially those with a smaller size, was completely dissolved. Of course, the amount of Nb which goes into solution is greater for steel B. This implies also that the amount that can be precipitated at lower temperature, as well as the driving force for this process to occur, are higher for this material.

Although no direct observation of the precipitation state in the HAZ is available, it is expected that, during the cooling stage of welding, the higher amount of Nb should produce an abundant precipitation of small and Nb-rich particles, similarly to what is found in the base metal, especially in association with the phase transformation from austenite to bainitic or acicular ferrite. The interaction between ferritic (or interphase) precipitation of Nb-Ti carbides and the austenite decomposition could be responsible for a greater microstructure refinement in steel B through a pinning effect on the moving boundaries of the bainitic ferrite.

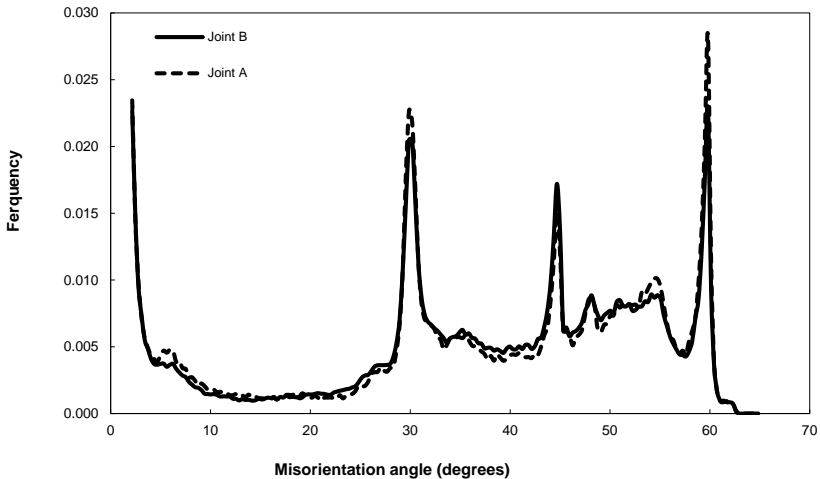


Figure 8. Misorientation distribution profile in CGHAZ by EBSD.

### Mechanical Properties

Tensile testing resulted in fractures far from the welded zone and the UTS was consequently satisfactory, Table III.

Hardness profiles (HV10) in the HAZ were measured near the Outer Diameter (1.5 mm from surface), mid thickness and near Inner Diameter (1.5 mm from surface). Recorded values as a function of the distance from the fusion line together with the corresponding range measured in Weld Metals (WM) and Base Metals (BM) are shown in Figure 9. It can be seen that the overmatching of the weld metal of both the joints and the reduced softening in the HAZ is consistent with the results of tensile testing. The hardness in the HAZ of the joint A is systematically slightly lower than that of the joint B (about 10 Vickers points) as a consequence of a less refined microstructure [5].

Charpy V transition curves are shown in Figure 10. Joint B results are almost fully ductile from a test temperature of -20 °C with corresponding good energy values (>200 J), while joint A shows a fully ductile behavior only at +20 °C. This different behavior can be explained in terms of the better refinement of the CGHAZ packet of joint B with respect to that of joint A [8].

Table III. Tensile Test Results for Joints A and B (average of two specimens)

|               | UTS<br>MPa | Fracture location |
|---------------|------------|-------------------|
| <b>Pipe A</b> | 696        | Base material     |
| <b>Pipe B</b> | 715        | Base material     |

The image displays four photographs of tensile test specimens, arranged in two pairs. The top pair is labeled 'Pipe A (0.07% Nb)' and the bottom pair is labeled 'Pipe B (0.10% Nb)'. Each pair shows a specimen before and after fracture. The fracture occurs in the base material, as indicated by the table above. The specimens are dark metal with a central necked region. The fracture surfaces are visible, showing a typical ductile fracture pattern with some dimpling.

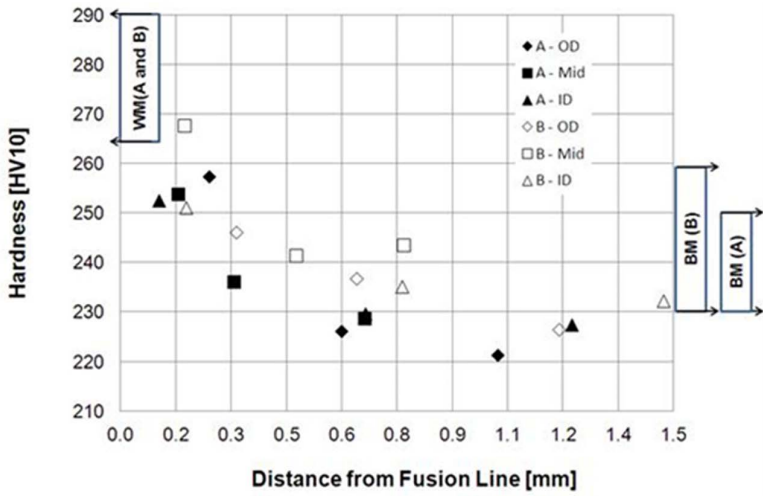


Figure 9. Hardness profiles in HAZ.

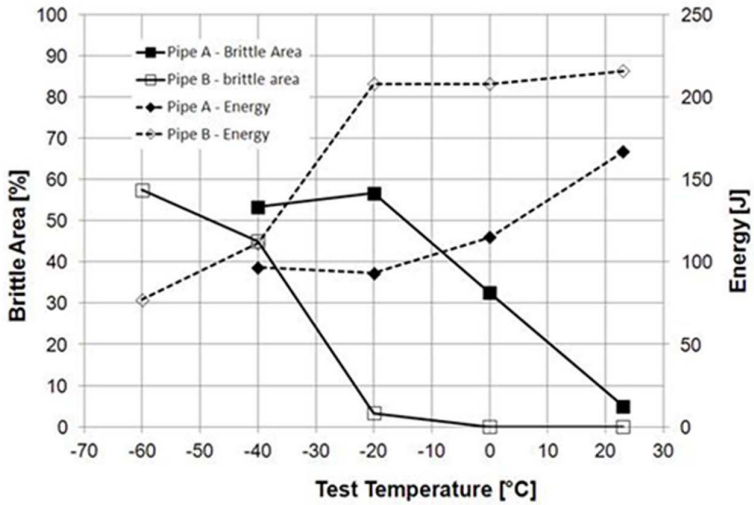


Figure 10. Charpy V transition curves (notch in fusion line).

## Conclusions

The effect of Nb content in the range 0.07%-0.10% on the HAZ microstructure of X80 large diameter pipes is reported in this paper.

As far as the base materials are concerned, both pipes are characterized by an acicular ferrite microstructure; the pipe with 0.07% Nb shows a coarser microstructure (larger packet size). Precipitates are mainly Nb/Ti carbides in both materials. Moreover, in the case of a higher Nb content, they are richer in Nb, and present in higher volume fraction.

Concerning the welded joint, results show that, although the small difference in Nb content is not able to affect the prior austenitic grain size, and therefore the local hardenability, it is still able to influence the size of the bainitic packet and of cells in the heat affected zone. Since these are the microstructural parameters affecting impact toughness and hardness behavior, such effects on microstructure reflect on mechanical behavior, showing an improvement of both toughness and hardness if higher Nb content is considered. In particular, the hardness in the HAZ of the lower Nb joint is systematically lower than the one with higher Nb content as a consequence of a less refined microstructure. Moreover, the higher Nb joint results are almost fully ductile starting from a test temperature of -20 °C with corresponding good energy values (>200 J), while the joint with lower Nb content does not show a fully ductile behavior below +20 °C.

## References

1. M. Hamada, Y. Fukada and Y. Komiz, "Microstructure and Precipitation Behavior in Heat Affected Zone of C-Mn Microalloyed Steel Containing Nb, V and Ti," *The Iron and Steel Institute of Japan International*, 35 (10) (1995), 1196-1202.
2. S.F. Medina et al., "Influence of Ti and N Contents on Austenite Grain Control and Precipitate Size in Structural Steels," *The Iron and Steel Institute of Japan International*, 39 (9) (1999), 930-936.
3. M. Chapa et al., "Influence of Al and Nb on Optimum Ti/N Ratio in Controlling Austenite Grain Growth at Reheating Temperatures," *The Iron and Steel Institute of Japan International*, 42 (11) (2002), 1288-1296.
4. P. Brozzo et al., "Microstructure and Cleavage Resistance of Low-Carbon Bainitic Steels," *Metal Science*, 11 (4) (1977), 123-130.
5. A. Di Schino, L. Alleva, and M. Guagnelli, "Microstructure Evolution During Quenching and Tempering of Martensite in a Medium C Steel" (Paper presented at the 4th Joint International Conference on Recrystallization and Grain Growth, Sheffield, UK, 2010), in press.
6. F. Fazeli et al., "Modeling the Effect of Nb on Austenite Decomposition in Advanced Steels" (Paper presented at the International Symposium on the Recent Development in Plate Steels, Winter Park, Colorado, USA, 2011).

7. C. Shiga, "Effect of Steelmaking, Alloying and Rolling Variables on the HAZ Structure and Properties in Microalloyed Plate and Linepipe" (Paper presented at the International Conference on the Metallurgy, Welding and Qualification of Microalloyed (HSLA) Steel Weldments, Houston, Texas, USA, 1990).

8. A. Di Schino and M. Guagnelli, "Metallurgical Design of High Strength/High Toughness Steels" (Paper presented at the Thermec 2011 International Conference, Quebec City, Canada, 2011), in press.